*Article*

# Device for Dual Ultrasound & Dry Needling Trigger Points Treatment

**Gerardo Portilla[1], Francisco Montero de Espinosa [1,*]**

[1]ITEFI-CSIC Spanish High Research Council, Serrano 144, Madrid, Spain

* Correspondence: francisco.montero@csic.es

**Abstract:** Ultrasound is a well-known tool to produce thermal and non-thermal effects on cells and tissues. These effects require a correct application of ultrasound in terms of localization and acoustic energy delivered. This article describes a new device that combines ultrasound and Dry Needling treatments. The ultrasound transducer can rotate in 3D space mechanically to align itself in the direction of the needle. The transducer electronically focuses the acoustic pressure automatically on the needle tip and its surroundings. A computer, using graphical interface software, controls the angulation of the array and the focus position.

**Keywords:** Ultrasound ; Physiotherapy ;Rehabilitation ; Dry Needling

## 1. Introduction

Physiotherapy and rehabilitation treatments with ultrasound have been performed for more than six decades. To date there is no proven agreement on the relationship between the doses applied in treatments and the therapeutic response in musculoskeletal diseases [1-4]. One of the problems to justify this is that the published studies refer to a wide range of diseases and therefore the doses of ultrasound are very varied. Ultrasound exposure produces various biological effects on cells and tissues. These effects are usually grouped into thermal and non-thermal to differentiate them since thermal effects are the most used in the first decades of the use of physiotherapeutic ultrasound due to the known relationship between energy absorption and heating of the medium [5-6]. The mechanical interactions between the pressure wave and the medium [7,8], such as cavitation produced by ultrasound not only in cells but also in vivo, cause changes at the cellular level that are the cause of cellular alterations that make possible the repair of musculoskeletal lesions [9,10]. One of the most commonly treated conditions is myofascial trigger points (MTPs) as they are a source of acute and chronic pain and can be disabling [11-14]. D. G. Simons el al define MTPs as "a hyperirritable point in a tight band of skeletal muscle that is painful on compression, stretch, overload, or tissue contraction, usually responding with referred pain felt at a distance from the point" [15]. Some studies referring to MTP ultrasonic physiotherapy treatments conclude that the acoustic parameters of the treatment have been misused. They conclude that a higher ultrasonic intensity than that used in most studies is needed to achieve beneficial effects [16]. Alexander LD et al. published the results of a systematic review on ultrasound treatments of shoulder soft tissues. In this work, the authors propose the use of an acoustic energy density higher than 400 J/cm2, justifying the futility of ultrasound claimed by some studies

 doi:10.20944/preprints202211.0446.v1



with the low energy used [17, 18]. Another central question that always remains in the mind of an expert in acoustic propagation is, did the programmed acoustic pressure of the commercial and laboratory devices used always reached the right place with the desired acoustic pressure? The medium is a finite structure full of geometrically complicated reflectors, not a semi-infinite homogeneous material as assumed in the Standards [19] .

Dry Needling (DN) is a treatment modality of chronic musculoskeletal pain used by physicians and physical therapists worldwide. It is based on the insertion of a thin needle through the skin to get to tender points in the body. Dry needling is defined by the American Physical Therapy Association as "a skilled intervention that uses a thin filiform needle to penetrate the skin, and stimulate underlying myofascial trigger points, muscular, and connective tissues for the management of neuromusculoskeletal pain and movement impairments" [20 ]. An excellent review of the history of DN was written by D.Legge [21]. Interestingly, the success of DN as a treatment of painful musculoskeletal disorders came up when observing that the effects obtained with the injection of different substances on the muscles- anti-inflammatories, anesthetic,..- was similar to the only insertion of a needle. In parallel with this fact, the explosion of the use of acupuncture to release pain in the 60's made that DN treatments, guided by musculoskeletal scientific and contrasted theory, grew rapidly to be at present a well-known and contrasted therapy. The most targeted DN treatments are myofascial trigger points (MTP). DN of MTP is not only a local treatment from the point of view of repairing a stressed muscle structure but it is also a treatment of a pain that is also reflected in points away from the MTP [22]. DN treatments have been shown to modify the composition of the chemical environment of the lesion and decrease the noise level of the endplates. However, the reason why an acupuncture needle produces this effect is not fully understood. [24-25].

Deep DN treatments for MPTs produce different effects. Contraction knots can be broken and contracted muscle bundles can be lengthened by reducing the overlap between actin and myosin filaments. Likewise, motor endplates can be destroyed by denervation the distal axons [25]. Mechanical, chemical, endocrinological, microvascular, neural and central effects have been reported [26].

It is interesting to note that in the DN treatments the exact point of the MTP is localized when the local twitch responses (LTR), which are involuntary spinal cord reflexes of the muscle fibers in a taut band, appears. This ensures that the tip of the needle is in the core of the MTP [27,28].

Few studies exist comparing DN with ultrasound treatments [29,30]. Interestingly, those existing compares DN with ultrasound Physiotherapy using ultrasound commercial systems but with high intensity levels. This ultrasound technique is call high-power pain threshold ultrasound (HPP-TUS) [31,32] .The treatment consists of, using continuous wave, gradually increase the intensity from the lowest intensity level to the intensity level at which the patient reports that the pain is not longer tolerable, maintaining the sonication a few seconds more.

The clinical treatment that we propose consists of a two steps actuation. First, the physiotherapist introduces a DN needle to locate and treat the trigger point performing well-known DN clinic procedures and then, leaving the needle in the body, the ultrasonic device is placed on the patient skin delivering focused ultrasound at the tip of de needle and surroundings to apply the programmed ultrasound treatment.

In the paper the design, realization and test of an ultrasonic device prototype to combine DN with ultrasound Physiotherapy is described.

## 2. Materials and Methods

### *2.1 Piezoelectric array transducers*

 doi:10.20944/preprints202211.0446.v1



In a previous paper, the authors presented a new device to perform focused physiotherapy with two ultrasonic array transducer designs [34]. The same concept is used in this work with the only difference that a hole is made at the center to permit the application of the array on the patient skin when the needle has been inserted in the body. Figure 1 shows two arrays design showing the central hole. The array made of concentric active elements permits to focus electronically along the propagation z-axis. The array made of a 2D distribution of active elements permits the electronic focusing in the entire 3D volume. Figure 2 shows the real array transducer.

Two different array transducers were fabricated. The 8 concentric array elements type and the 2D 28-elements type were made with the aperture designs of Figure 1. The fabrication technique is described in [33]. Before fabricating the piezocomposite 1-3 discs, a bore was made at the center of the piezoceramic discs with a diamond hollow drill – Diamond Board- using a high-speed drill - TV-4 Maquimetal-.

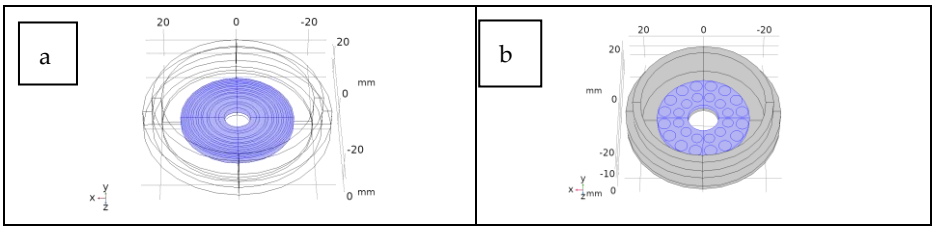


**Figure 1.** Drawings of the concentric elements array- a- and 2D 28-elements array – b-.

*2.2 Electrical excitation*

A commercial multi pulser with programmable excitation frequency, output voltage and channel excitation delays was used (SITAU, DASEL SL). The channel output electrical signal is a 0-150V programmable unipolar negative square pulse. The pulser power source and the power transistors limit the number of cycles and pulse repetition rate. All the engineering and user software applications were made with LabView (National Instruments Inc.).

*2.3 Acoustic field simulation*

COMSOL 5.3 (COMSOL Inc.) was used to simulate the vibration performance and the acoustic field of the transducers to take into account the non-homogeneous amplitude and phase vibration of the array elements and the appearance of structural resonance modes. The material parameters used in the simulation are the same as those used in Portilla et al [33].

*2.4 Transducer test*

The array transducers were tested including the measurements of the input electrical impedance of the array elements, the mechanical vibration profile at the emission face in air and the acoustic diffraction field in water. The transducer elements input electrical impedance was measured with an impedance analyzer (4294A Agilent). The mechanical vibration pattern was tested in air coupling with a vibrometer – ( Polytec OFV 5000/505). A water tank with computerized 3D cartesian stages- 50 ⊚m precision- and a PVDF needle hydrophone (Dapco V-19-T, 0,6mm active head diameter) were used to perform the acoustic field measurements.

Preprints (www.preprints.org) | NOT PEER-REVIEWED | Posted: 23 November 2022 doi:10.20944/preprints202211.0446.v1



## 3. Results

### *3.1 Acoustic field simulation and measurement*

#### *3.1.1. 8-elements annular array transducer*

After testing the vibration pattern of the arrays, the acoustic field of the two arrays was calculated and measured at different focus positions. Figure 2 shows, as example, the calculated and measured diffraction field in the zy plane of the 8-concentric elements array vibrating at f=640 kHz at the programmed focus positions F(x,y,z)= (0,0,30)mm and F(x,y,z)= (0,0,50) mm .

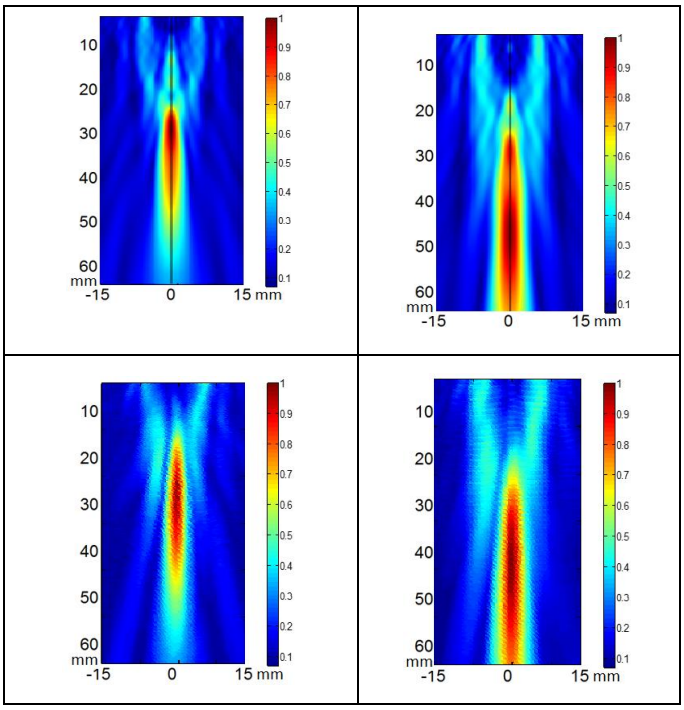


FIGURE 2.- Acoustic pressure field in the zy plane of the 8 elements annular array transducer when excited at 640 kHz with electronic focus at F(x,y,z)= (0,0,30) mm and F(x,y,z)= (0,0,50) mm . Left column focus position at F(x,y,z)= (0,0,30) mm, right column focus position at F(x,y,z)= (0,0,50) mm. Rows up to bottom show the COMSOL simulation and the experimental result respectively.

Rows up to bottom show the COMSOL simulation, and the experimental result respectively. Linear propagation and no attenuation were considered. Left column focus position at F(x,y,z)= (0,0,30) mm, right column focus position at F(x,y,z)= (0,0,50) mm . Relative scales are used.

Figure 3 shows the comparison of the 8-elements concentric array calculated acoustic diffraction parameters with the experimental ones. The calculations were made for eight focus distances from F=30mm to F=80 mm. The measurements include three focal distances F=30 mm, F= 50mm and F=70 mm. Both the calculated and the measured acoustic pressure values are relative to the respective acoustic pressure maximum value. The measured relative acoustic pressure at the focus agrees better with the FEM simulation.

Preprints (www.preprints.org) | NOT PEER-REVIEWED | Posted: 23 November 2022 doi:10.20944/preprints202211.0446.v1



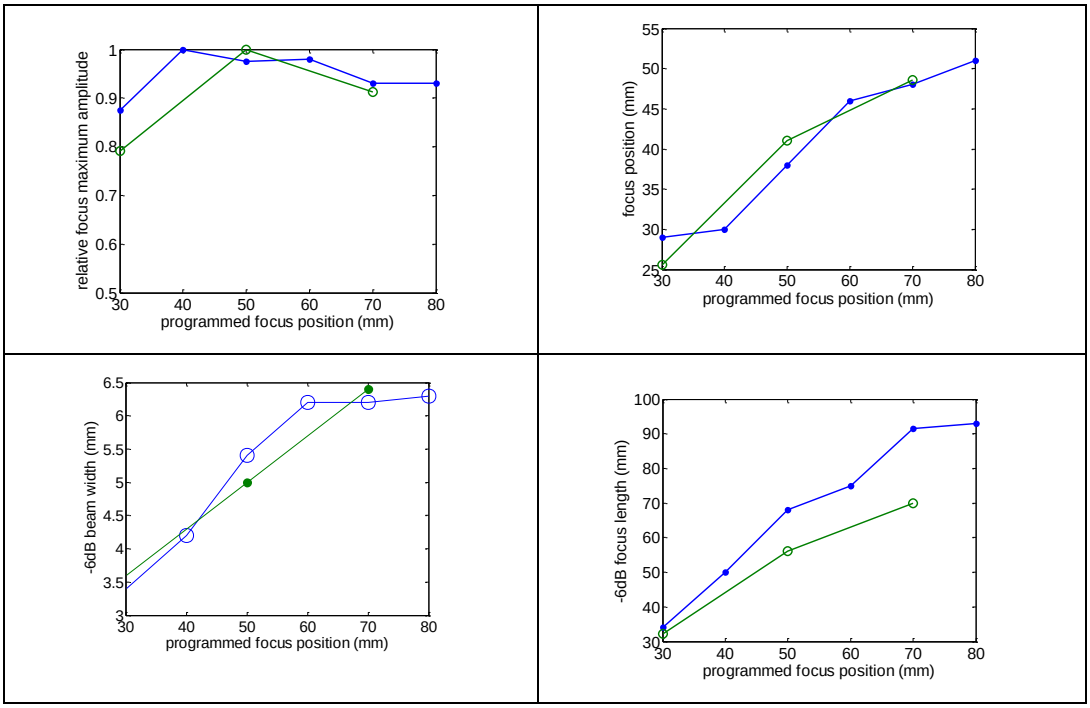


FIGURE 3 .- Comparison of the calculated – green line- and measured - blue line-acoustic diffraction parameters of the 8-elements concentric array . Frequency f= 640 kHz.

The disagreement between the FEM-COMSOL and the experimental results can be justified due to the imperfections in the construction of the transducer – adhesive interface- and the consideration of the piezocomposite as a homogeneous material.

Concerning the calculated absolute acoustic pressure and considering tissue attenuation a=11.55 Np/m , pressure amplitude around 2 MPa can be ideally obtained at a depth range between 30 mm and 50mm in muscle tissue with an electric excitation voltage V=40 Vp .

*3.1.2 2D 28-elements array transducer*

The acoustic pressure diffraction field of the 2D-28 elements array transducer was also calculated with the same attenuation coefficient a=11.55 Np/m and electric amplitude voltage signal V=40 Vp. Resonance frequency f=860 kHz. Figure 4 second row shows the acoustic pressure diffraction at the focus positions F=30 mm and F=40mm without electronic steering. Compared with the same programmed position focus for the 8 concentric elements array, the acoustic pressure level is more than four time less. The reason, independently that the diffraction aperture is different – concentric annular elements versus circular elements-, is the decrease of active emission surface. Nevertheless, the 2D aperture design permits electronic steering. Figure 4, third and fourth rows, show the electronic steered acoustic diffraction up to 10 mm along the y axis. As observed, pressure maximum decreases with the deflection angle – up to a 30%- and the focus distance- 10%-.

The ellipsoid length increases 80% with the focus distance as expected. The width also increases up to 50%. The increase of the deflection angle brings out the strength of the grating lobes at the volume closer to the transducer emission surface. This effect is bigger for shorter focus distances.

Preprints (www.preprints.org) | NOT PEER-REVIEWED | Posted: 23 November 2022 doi:10.20944/preprints202211.0446.v1



| mm | z=30 | z=40 |
|---|---|---|
| x=0<br>y=0 | 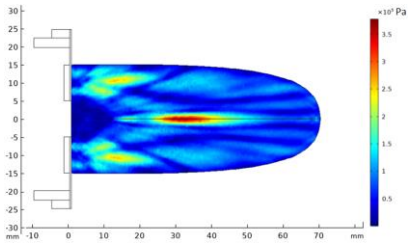 | 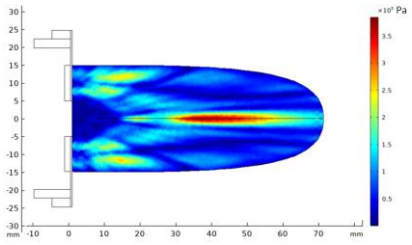 |
| x=5<br>y=0 | 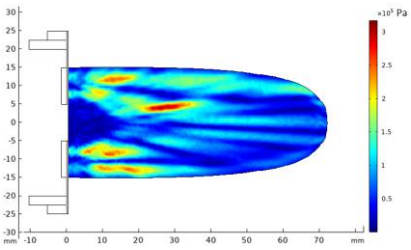 | 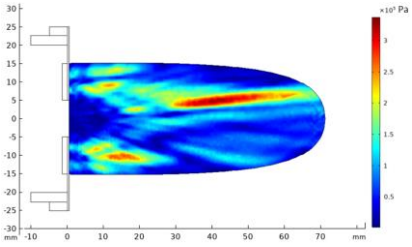 |
| x=10<br>y=0 | 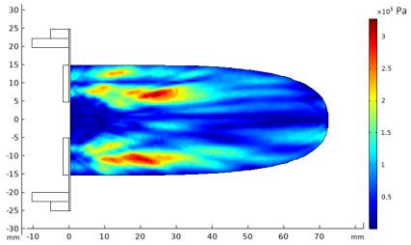 | 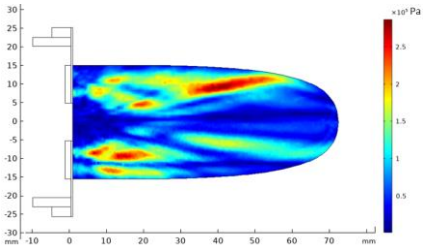 |

FIGURE 4.- FEM_COMSOL calculated acoustic diffraction field of the 28-elements 2D array. Resonance frequency f=860 kHz. First column, (x,y) focus coordinates. Upper row, z focus coordinates.

The acoustic pressure diffraction was calculated when steering electronically the 2D-24 elements array transducer at two (x,y,z) focus positions: (5,5,40) mm and (10,10,40) mm. The excitation voltage was V=40 Vp and an attenuation coefficient a=11.55 Np/m was used. As seen in Figure 5 , referring to the non steered case xyz =0,040)mm, the pressure maximum at the focus locus decreases 15% at (5,5,40) mm- 7mm from the xyz=(0,0,40)mm- and 35% at (10,10,40) mm - 14 mm from (0,0,40) mm-. Grating lobes increase their relative amplitude from less than 28% without electronic steering up to

| a) | b) |
|---|---|

 doi:10.20944/preprints202211.0446.v1



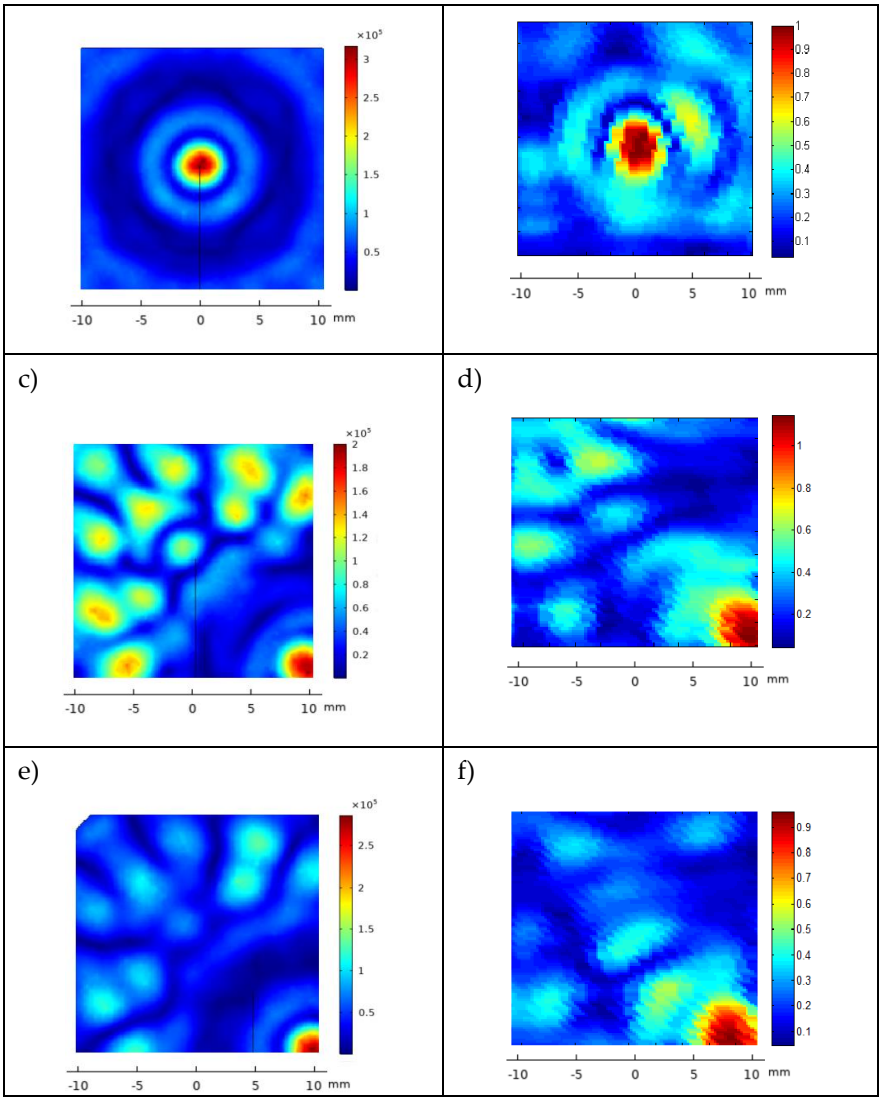


FIGURE 5.- FEM_COMSOL acoustic pressure diffraction field of the 2D-28 element array excited at f=860 kHz. XY plane. Left column, from top to bottom the calculated acoustic diffraction in focus coordinates (x,y,z)=( 0,0,40) mm , (x,y,z)=(10,10,40) mm and a translation of coordinates (x,y,z) =(5,5,40)mm from the focus case (x,y,z) =(5,5,40)mm. The right column, from top to bottom, shows the focused acoustic diffraction measured at (x,y,z)=( 0,0,40) mm , (x,y,z) =(10,10,40) mm and the result of combining the mechanical steering at (x,y,z) =(5,5,40) mm plus the electronic steering at (x,y,z) =(5,5,40)mm. The scale of the measured acoustic pressure is relative to the maximum pressure at (x,y,z) =(0,0,40) mm.

70% when steering at (10,10,40) mm. At the intermediate position (5,5,40) mm, the grating lobes maximum amplitude have a relative pressure of 48% respect to the focus acoustic pressure. If a sonication security zone is defined where the acoustic pressure be less than -6dbs the maximum lobe acoustic pressure [32] , the (10,10,40) mm electronic steering should be prohibited. The solution is to combine the mechanical and the electronic steering. The (10,10,40) mm focus position can be attained moving first the transducer mechanically to the (5,5,40) mm position, steering then electronically the pressure lobe another incremental (5,5,40) mm – Figure 5e-. Figures 5b,5d and 5f show the corresponding experimental acoustic diffraction pressure of the simulated focus coordinates.

Preprints (www.preprints.org) | NOT PEER-REVIEWED | Posted: 23 November 2022 doi:10.20944/preprints202211.0446.v1



### 3.2 . *Device and software*

A new device was developed to apply focused ultrasound at the tip of a DN needle introduced in the body following a simple procedure - Figures 6a and 6b-. The device consists of a manipulator - Figure 6 c2 -with a needle angle IMU gauge – Figure 6 c1 - plugged to a computer, a multi-pulser, and a graphic interface software. The software was made in a format preferably compatible with Windows but can be adapted to any other operating system -Figure 7-.

The manipulator has an actuator with a spherical parallel robot with two degrees of freedom to steer mechanically the array transducer –Figure 6e-. This robot has two coplanar servomotors - SG90 Tower Pro- acting in a parallel mechanism, which rotates the ultrasonic array transducer in such a way that the acoustic diffraction lobe can be scanned in the 3D space – Figure 6 e7-. A cavity filled with a gel in between the transducer array and the skin permits the coupling of the transducer as it is rotated -Figure 16 e8-.

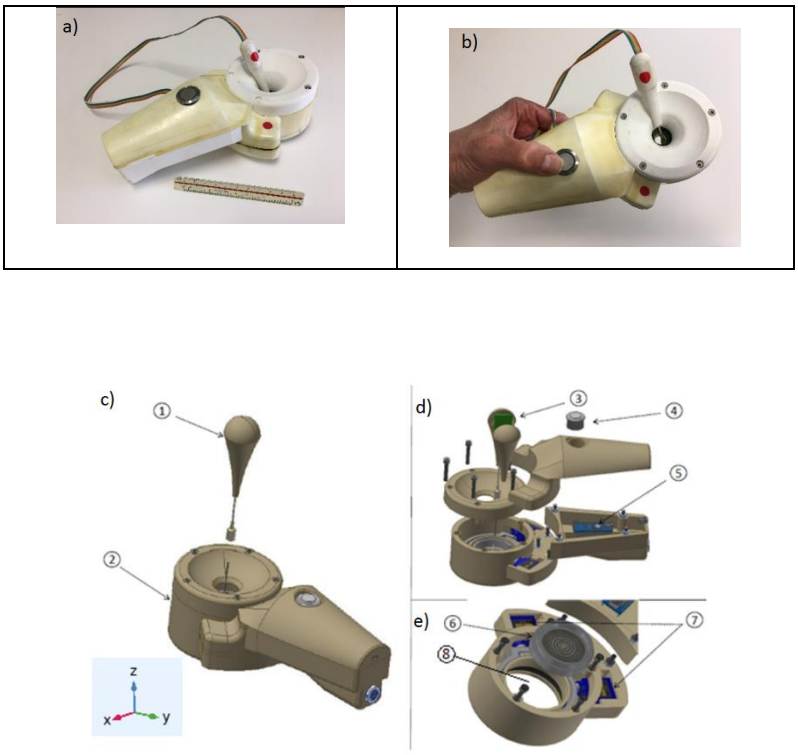


FIGURE 6.- Manipulator prototype with the needle angle gauge- a) and b). c) Prototype description showing the needle angle sensor-1- , the manipulator-2- and the reference geometric coordinates. d) Inertial sensor IMU -3-, main operation switch -4- and microprocessor- 5-. e) Array transducer before been introduced in the parallel robot -6- , parallel robot -7- and gel cavity-8-.

The purpose of the actuator 3D rotation is to orientate the array transducer to locate it in the plane perpendicular to the needle axis. So, a senor to know the angulation of the needle having as reference the manipulator application plane – XY plane of Figure 10- is needed. This sensor has a tube and an inertial sensor -Figure 6 d3- connected to a microprocessor –Figure 6 d5-. The microprocessor is connected to a PC computer via USB. When the sensor tube is introduced in the needle section which remains out of the body after the puncture, the acceleration variables measured by the inertial sensor are calculated in the microprocessor and read by the computer, calculating the real inclination of

Preprints (www.preprints.org) | NOT PEER-REVIEWED | Posted: 23 November 2022 doi:10.20944/preprints202211.0446.v1



the needle using the formulas of equation (1) [34-36]. To determine the position of the needle tip, the microprocessor executes the rotation matrix equation (2) [37-39]. $z_n$ is the length of the needle section inserted into the body, a parameter that must be introduced previously in the software interface by the physiotherapist. An action switch placed in the manipulator- Figure 6 d4- activates the 2D rotation movement of the parallel robot orientating the array in the needle direction.

$$\theta_x = arctan\left(\frac{a_x}{\sqrt{a_y^2+a_z^2}}\right) \phi_y = arctan\left(\frac{a_y}{\sqrt{a_x^2+a_z^2}}\right) \quad (1)$$

$$\begin{bmatrix} x \\ y \\ z \end{bmatrix} = Rotx(\theta)Roty(\phi)\begin{bmatrix} 0 \\ 0 \\ z_n \end{bmatrix} \quad (2)$$

The coordinates ( $x, y, z$ ) are the position of the needle tip relative to the center of the parallel robot. Once the coordinates of the needle tip are known, the software calculates the time delays of the electric excitation of all the array transducer elements to focus the ultrasonic field at the needle tip coordinates. The transducer frequency, propagation velocity and signal excitation parameters as excitation voltage, number of cycles, pulse repetition rate and treatment time must be introduced previously in the graphic interface software –Figure 7-.

The graphic interface software has three XY charts with a red spot- Figure 7-. The upper left chart is used to select the electronic (x,y) steering coordinates. A circle shows the limit to the appearance of acoustic pressure zones with a pressure bigger than the -6dB the maximum of the acoustic pressure at the focus -1-. Two linear cursors can be moved to position the red point that represents the desired electronically steered focus position -2-. The down left chart is used to show the position of the acoustic focus when being steered mechanically.

The mechanical steering can be introduced manually for engineering test-3- or automatically using the needle angle sensor for clinical purposes -4-. The upper right chart shows the result of the mechanical and electronic steering combination -6-. The value of the needle length inserted should be introduced manually -7-. The three green action buttons at the left activate pre-programmed ultrasonic treatments -8-. The clinic treatment start&stop activation can be made with the switch located in the manipulator or with the software graphical switches -9-.

Preprints (www.preprints.org) | NOT PEER-REVIEWED | Posted: 23 November 2022 doi:10.20944/preprints202211.0446.v1



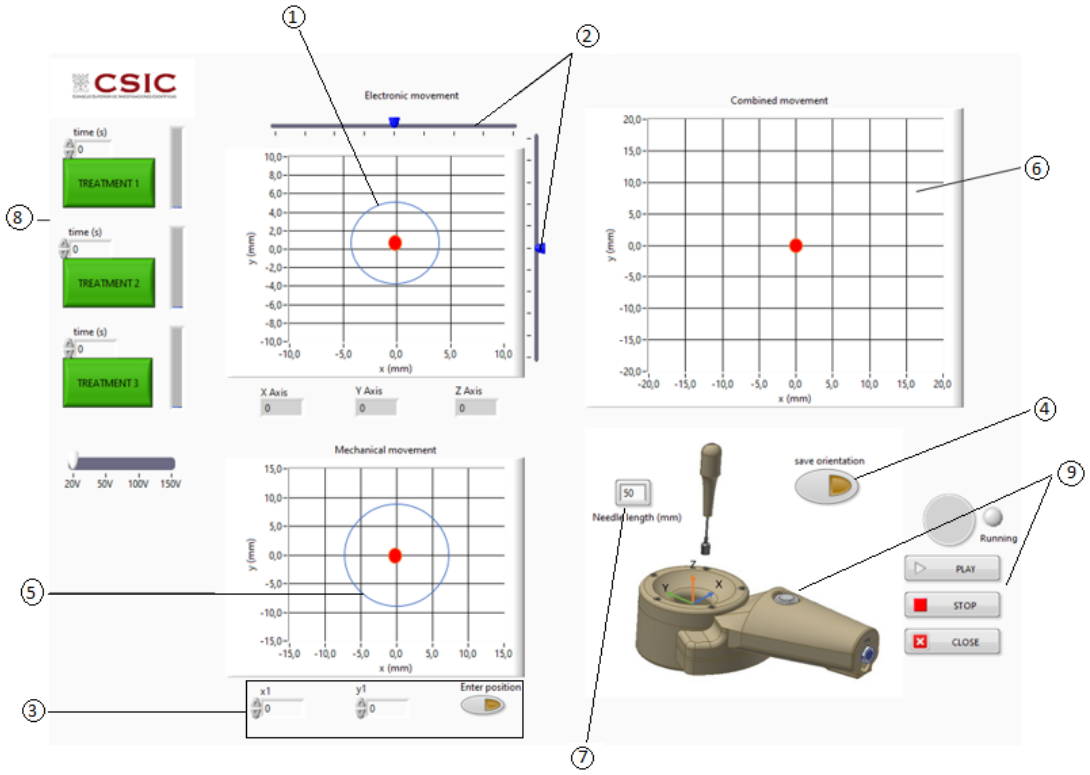


FIGURE 7.- User graphic interface.1) Electronic steering : limit to get grating or diffraction lobes with an acoustic pressure bigger than -6dB the maximum of the acoustic pressure at the focus . 2) Electronic steering linear cursors. 3) Manual introduction of the mechanical steering focus position. 4) Automatic positioning of the mechanical steering using the needle angle sensor. 5) Mechanical steering: limit to get grating or diffraction lobes with an acoustic pressure bigger than -6dB the maximum of the acoustic pressure at the focus. 6) Combination of the mechanical and electronic steering. 7) Needle inserted section. 8) Pre-programmed ultrasonic treatments. 9) Start&stop activation.

### *3.4 Clinical procedure*

Figure 8 shows the proposed clinic procedure. It consist of, firstly, the localization of the MTP in the patient body by the clinician– Figure 8a , MPT of 5mm x 20mm at 50 mm from the skin-. Then, the needle is punctured through the skin and manipulated following known clinical procedures performing DN aimed to deactivate the MPT -Figure 14b- . After the DN treatment, the needle must be left in the patient body such that its tip be as close as possible to the MPT volumetric centre. A thick layer of ultrasound gel should be applied to the skin around the needle –Figure 8c, 5-. The next step is to place the transducer on the patient body introducing the needle through the central transducer hole – Figure 8c, 4-. The clinician must introduce the needle incision depth on the corresponding graphic interface window – Figure 12,7- . Next, the angle gauge is coupled to the needle and by pressing the activation "on" button of the manipulator, the transducer rotates mechanically – Figure 14d- and starts the programmed ultrasonic treatment focusing the acoustic pressure on the needle tip- Figure 14e,6-. The acoustic diffraction lobe dimensions shown in the figure have those of the 8-concentric elements array focused at (0,0,50) mm. The manipulator should be maintained fixed to the patient body during all the ultrasonic treatment.

 doi:10.20944/preprints202211.0446.v1



As seen in Figure 8e the intersection of the acoustic pressure lobe, that has a pressure value higher than -6 dB the pressure maximum, and the MTP does not cover the entire volume of the MPT. To sonicate the entire MTP volume, if necessary, the 2D array transducer is the most appropriated design because the acoustic diffraction lobe can then be electronically steered. As simulated in figures 4, 8f and 8g, the acoustic pressure lobe can be deflected electronically from the needle tip position as much as +/- 10mm from the focus location - needle tip- without decreasing the acoustic pressure more than 25 %.

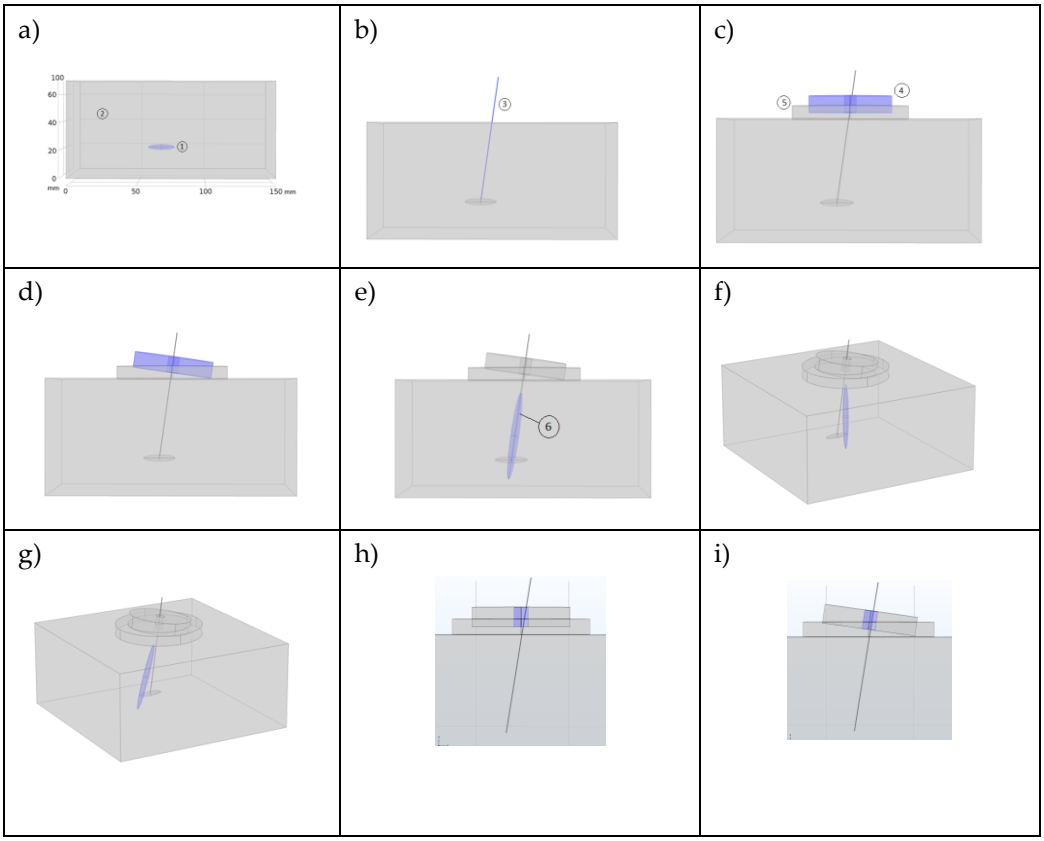


FIGURE 8.- Graphical representation of the clinical procedure :a) MTP localization, b) needle insertion, c) transducer application, d) transducer mechanical steering at the needle angular orientation, e) focused sonication , f) and g) electronic steering ,h) and i) maximum needle angulation permitted for the 8 concentric elements prototype.

*3.3 Mechanical steering accuracy test*

The mechanical angular steering accuracy of the device was tested with an experiment that reproduces the clinical procedure. A cylindrical piece was placed on the transducer hole coaxial with the transducer z axis to house on it a 650 nm laser diode with a lens - focus diameter of 3 mm with a divergence angle of 0.019 degrees- illuminating in the forward transducer direction – (0,0,-z) direction-. A thin metallic bar coaxial with the laser beam was also housed in the rear direction – (0,0,z) direction-. A screen with millimetre scale was placed parallel to the manipulator emission plane

 doi:10.20944/preprints202211.0446.v1



at a distance of z= 500 mm .Different (x,y,500) mm transducer mechanical steered positions are introduced in the corresponding software window –figure 7,3-. Inserting the IMU in the metallic bar, the roll and pitch degrees are obtained. The microprocessor calculates the laser spot position in the (X,Y,500) mm plane and then the robot is automatically rotated, moving the laser spot. The (x,y) positions of the laser spot in the screen are then measured. The absolute error of the measured position depends on the direction of the angulation - pitch and roll - indicating that the structure of the parallel robot has some construction imperfections. The error is larger for shorter angulations, which is compatible with the type of stepper motor used. The mean absolute error is Av(x,y)= (0.37,0.4) mm. Importantly, the error is less than 16% of the narrowest focus width tested with the 28-element, 860 kHz 2D array transducer.

## 5. Conclusions

The needle angulation is a critical parameter. The larger the bore diameter, the smaller the emission aperture of the entire transducer. The smaller the bore diameter, the smaller the maximum needle angulation permitted. If the present transducer designs are taken as a reference, the maximum needle angle permitted is +/-9 degrees for the case of the 8-concentric elements - 7 mm diameter center hole- and +/-14 degrees for the case of the 28-eñements 2D array – 10mm diameter center hole -. Figures 8h and 8i show the angulation limit for the case of the 8 concentric elements array prototype.

The calculated pressure maxima at the focus when exciting the array transducers with a monochromatic voltage V=40Vp are close to 2Mp for the case of the 8 concentric elements design and close to 0.4 MPa for the case of the 28 elements 2D array design. Voltage sources higher than 120Vp should be then used if treatments aimed to apply short pulses of acoustic pressure higher than 1 MPa are needed [40,41].

Different array apertures can be designed to increase the acoustic pressure output efficiency. For instance, by only using a piezoelectric ring with 40 mm external diameter and an aperture design of 48 sectorial elements leaving the same capsule design, the calculated acoustic pressure at the focus is more than twice that of the 24- elements 2D prototype with the same excitation voltage.

As mentioned in [33], the objective pursued when developing focused ultrasonic systems for Physiotherapy is to reach the area of the musculoskeletal lesion, and only this area, with the acoustic pressure necessary to promote thermal or non-thermal effects depending on the pressure and time-averaged intensity. Using a needle to reach the lesion, as it is done when using DN, opens up the possibility of knowing the relative coordinates of the lesion in relation to the needle puncture location. By measuring the depth of the puncture and the polar angles of the needle, the lesion is then localized in 3D and the transducer can be oriented mechanically and/or electronically to deliver the desired acoustic treatment to the target. Moreover, the use of array transducers makes it possible to scan the lesion in a controlled manner. The combination of mechanical and electronic expands the body volume to safely deliver the ultrasound dose while keeping the applicator fixed on the patient's skin.

The ultrasound dose can be programmed in treatment time, acoustic pressure, acoustic intensity and position guided with the user graphic interface. The proposed device is designed to get relative high pressure ultrasonic to explore the action of non-thermal effects.

The parallel robot of the current prototype can be upgraded to achieve higher motion accuracy with better stepper motors and by machining the parallel mechanism instead of using 3D printing.

By way of summary, a prototype device has been described to show how DN can be combined with focused ultrasound in a very simple way for use by physiotherapists and rehabilitators. All subsystems of this device mainframe-

aperture and frequency of the transducer array, number of elements, acoustic pressure and delivered acoustic intensity, mechanical angulation of the transducer,.. - can be redesigned according to clinical needs.

.

**Author Contributions:**

Conceptualization, 50.50; methodology, 50.50.; software, 100.0.; validation, 20.80,formal analysis, 20.80.; investigation, 10.90.; resources, 20,80.; data curation, 10.90.; writing—original draft preparation, 10.90.; writing—review and editing, 10.90.; supervision, 10.100.; project administration, 0.100.; funding acquisition, 0.100.

All authors have read and agreed to the published version of the manuscript.

**Funding:** This research was funded by SPANISH RESEARCH AGENCY, MINISTRY OF SCIENCE AND TECHNOLOGY, grant number DPI2016-80254-R.

**Data Availability Statement:** Not applicable.

**Acknowledgments:** The authors would like to thank Prof. José Ríos and Prof. Pablo Herrero for their expertise on Ultrasound Physiotherapy and Dry Needling.

**Conflicts of Interest:** The authors declare no conflict of interest.

## References

1. Erikson K, Fry F, Jones J. Ultrasound in Medicine-A Review, *IEEE Transactions on Sonics and Ultrasonics*, 1974 ;21(3):144–170.
2. Miller D, Smith N, Bailey M, Czarnota G, Hynynen K, MakinI. Overview of therapeutic ultrasound applications and safety considerations ,*J. Ultrasound Med.*, 2012;vol. 31(4): 623-634..
3. ter Haar G, DysonM., Oakley E.M.. The use of ultrasound by physiotherapists in Britain, *Ultrasound Med. Biol.* 1985;13:659–663.
4. Pope G.D., Mockett SP , Wright JP., A survey of electrotherapeutic modalities: ownership and use in the NHS in England, *Physiotherapy*. 1995; 81 (2):82–91.
5. Paliwal S, Mitragotri S . Therapeutic opportunities in biological responses of ultrasound, *Ultrasonics* .2008; 48(4): 271-278.
6. Szabo T, Ultrasound-induced Bioeffects In: *Diagnostic Ultrasound Imaging: Inside Out*. Elsevier: 2014: 653-697.
7. ter Haar G. Ultrasound bioeffects and safety. *Proc. IMechE* ; 224 Part H: J. Engineering in Medicine:363-373. DOI: 10.1243/09544119JEIM613.
8. Hill CR, Bamber JC , ter Haar G. In :*Physical Principles of Medical Ultrasonics* .John Wiley & Sons, Ltd; 2004.
9. Webster D, Pond J, Dyson M, Harvey W. The role of cavitation in the in vitro stimulation of protein synthesis in human fibroblasts by ultrasound. *Ultrasound in Med. and Biol.* 1978;4, :343-351.
10. Holland Ch K, Deng Ch X, Apfel RE, Alderman JL, Fernandez L A , Taylor KJW. Direct evidence of cavitation *in vivo* from diagnostic ultrasound. *Ultrasound in Medicine & Biology*. 1996;22,7: 917-925.
11. Fernández de Las Peñas C, Simons D, Cuadrado ML , Pareja. The role of myofascial trigger points in musculoskeletal pain syndromes of the head and neck.*J.Curr Pain Headache Rep*. 2007;11(5):365-72.
12. Lavelle E D, Lavelle W , Smith H S. Myofascial Trigger Points, *Anesthesiology Clinics*. 2007;25,4: 841-851.
13. Dommerholt B C, Stegenga J, Wensing B, Oostendorp M , High prevalence of shoulder girdle muscles with myofascial trigger points in patients with shoulder pain. *BMC Musculoskelet. Disord*. 2011;12, 139.
14. Bron C, Dommerholt JD, Etiology of Myofascial Trigger Points. *Curr Pain Headache Rep* .2012;16:.439–444. https://doi.org/10.1007/s11916-012-0289-4.
15. Simons D G, Travell J G, Simons L S . *Myofascial Pain and Dysfunction, The Trigger Point Manual*, 2nd ed. (2 Volumes). Ed. Williams & Wilkins, Baltimore, MD; 1999.
16. Majlesi J , Ünalan H . High-Power Pain Threshold Ultrasound Technique in the Treatment of Active Myofascial Trigger Points: A Randomized, Double-Blind, Case-Control Study. *Arch Phys Med Rehabil* .2004; 85:833-836.
17. Alexander LD, Gilman DR, Brown DR, Brown JL , Houghton PE. Exposure to low amounts of ultrasound energy does not improve soft tissue shoulder pathology: a systematic review. *Phys Ther.* 2010;90(1):4–25.

18. Ainsworth R, Dziedzic K, Hiller L, Daniels J, Bruton A, Broadfield J .A prospective double blind placebo controlled randomized trial of ultrasound in the physiotherapy treatment of shoulder pain. *Rheumatology*. 2007;46: 815–820.
19. Hekkenberg RT. .Characterising ultrasonic physiotherapy systems by performance and safety now internationally agreed. *Ultrasonics*. 1998;36 :713-720.
20. Gattie E , Cleland JA, Snodgrass S. A survey of American physical therapists' current practice of dry needling: Practice patterns and adverse events. *Musculoskelet Sci Pract*. 2020;50:102255.
21. Legge D. A History of Dry Needling. *Journal Of Musculoskeletal Pain*, 2014; Early Online: 1–7. DOI: 10.3109/10582452.2014.883041.
22. Dommerholt J. , Fernández De Las Peñas C. Basic concepts of myofascial trigger points (trps)," in "Trigger Point Dry Needling. An Evidence and Clinical-Based Approach. Ed ELSEVIER, second edition. 2018. : 3–19. ISBN: 9780702075186.
23. Dommerholt J, Fernández De Las Peñas C. Proposed mechanisms and effects of trigger point dry needling. In: *Trigger Point Dry Needling. An Evidence and Clinical-Based Approach.* Ed ELSEVIER, second edition.2018: 20–27. ISBN: 9780702075186.
24. Mann F. *Non-existent acupuncture points. Reinventing Acupuncture,* Ed. Butterworth-Heinemann, second edition, UK, London, 2000. ISBN13 9780750648578.
25. Gaspersic R, Koritnik B, Erzen I, Sketelj J. Muscle activityresistant acetylcholine receptor accumulation is induced in places of former motor endplates in ectopically innervated regenerating rat muscles. *Int J Dev Neurosci.*2001; 19(3): 339-46.
26. Dunning J, Butts R, Mourad F, Young I, Flannagan S, Perreault T . Dry needling: a literature review with implications for clinical practice guidelines. *Phys Ther Rev.* ,2014; 19(4):252–265.
27. Dexter JR , Simons G. Local twitch response in human muscle evoked by palpation and needle penetration of a trigger point. *Arch. Phys. Med. Rehabil*. 1981;62: 521.
28. Ga H, Koh HJ, Choi JH , Kim CH. Intramuscular and nerve root stimulation vs lidocaine injection to trigger points in myo-fascial pain syndrome. *J. Rehabil. Med.* 2007;39: 374–378.
29. Aridici R , Yetisgin A, Boyaci A, Bozdogan E , Dokumaci DS, Kilicaslan N, Boyaci N . Comparison of the Effi-cacy of Dry Needling and High-Power Pain Threshold Ultrasound Therapy with Clinical Status and Sonoelastography in Myofascial Pain Syndrome .*Am J Phys Med Rehabil*. 2016;95(10):149-158.
30. Ali HA, Elzohiery AK, Arafa MM , Elkadery NA .Dry needling versus ultrasonic in treating cervical myofascial pain syndrome . *QJM: An International Journal of Medicine*, 2020; 113, (1):222.
31. Kim Y, Yang HR, Lee JW , Yoon B CH. Effects of the high-power pain threshold ultrasound technique in the elderly with latent myofascial trigger points: A double-blind randomized study. *Journal of Back and Musculoskeletal Rehabilitation*. 2014;27:17–23.
32. Unalan H, Majlesi J, Aydin FY, Palamar D, Eryavuz M. High power pain threshold ultrasound therapy is as effective as local anaesthetic injection in the treatment of active myofascial trigger points. *European Journal of Pain*. 2006; 10 (S1):216.
33. Portilla-Tuesta G , Montero de Espinosa F. System and method for applying physiotherapeutic focused ultrasound. *Ultra-sonics*, 2022;121:106693.
34. Barbour N, Schmidt Ge, Inertial sensor technology trends . *IEEE Sensors journal*. 2001;l. 4:332-339 .
35. Neville CH, Ludlow C , Rieger B. Measuring postural stability with an inertial sensor: validity and sensitivity. *Medical devices*. 2015; 8: 447-455.
36. Mooney R, Corley G , Godfrey A, Quinlan LR, ÓLaighin G. Inertial sensor technology for elite swimming perfor-mance analysis: A systematic review. *Sensors(Basel)*.2016; 16( 1): 18.

37. Portilla G , Saltarén R, Rodríguez A, Cely J , Yakrangi O. A sensor based on a spherical parallel mechanism for the measurement of fluid velocity: experimental development. *IEEE Access*.2019; 7: 16145-16154.
38. Shepperd S W, Quaternion from rotation matrix. *Journal of guidance and control*. 1978; 1(3) : 223-224.
39. Slabaugh G. Computing Euler angles from a rotation matrix. Technical report. University of London (1999) ,htpp://ateseerx.ist.psu.edu/viewdoc/summary: doi: 10.1.1.371.6578.
40. Ronda S, Fernández M, San Román J, Montero de Espinosa F. Effects of Non-thermal Ultrasound on a Fibroblast Monolaye Culture: Influence of Pulse Number and Pulse Repetition Frequency ,*Sensors (Basel)*. 2021;21(15):5040, doi: 10.3390/s21155040.
41. Daniele de Oliveira P , Poli-Frederico RC, Pires-Oliveira D , Beltrão F, Shimoya-Bittencourt W, Martins-Santos V, Medeiros J, Franco de Oliveira R. Anti-Inflammatory and Healing Effects of Pulsed Ultrasound Therapy on Fibroblasts. *Am J Phys Med Rehabil*. 2020;99(1): 19-25.